

SocialNav: Training Human-Inspired Foundation Model for Socially-Aware Embodied Navigation

Ziyi Chen^{1*} Yingnan Guo^{1,2*} Zedong Chu^{1†} Minghua Luo¹ Yanfen Shen¹
Mingchao Sun¹ Junjun Hu¹ Shichao Xie¹ Kuan Yang¹ Pei Shi¹ Zhining Gu¹
Lu Liu¹ Honglin Han¹ Xiaolong Wu¹ Mu Xu¹ Yu Zhang² Ning Guo¹

¹Amap, Alibaba Group, China

²Zhejiang University, China

Abstract

Embodied navigation that adheres to social norms remains an open research challenge. Our **SocialNav** is a foundational model for socially-aware navigation with a hierarchical "brain-action" architecture, capable of understanding high-level social norms and generating low-level, socially compliant trajectories. To enable such dual capabilities, we construct the SocNav Dataset, a large-scale collection of 7 million samples, comprising (1) a Cognitive Activation Dataset providing social reasoning signals such as chain-of-thought explanations and social traversability prediction, and (2) an Expert Trajectories Pyramid aggregating diverse navigation demonstrations from internet videos, simulated environments, and real-world robots. A multi-stage training pipeline is proposed to gradually inject and refine navigation intelligence: we first inject general navigation skills and social norms understanding into the model via imitation learning, and then refine such skills through a deliberately designed Socially-Aware Flow Exploration GRPO (SAFE-GRPO), the first flow-based reinforcement learning framework for embodied navigation that explicitly rewards socially compliant behaviors. SocialNav achieves **+38% success rate** and **+46% social compliance rate** compared to the state-of-the-art method, demonstrating strong gains in both navigation performance and social compliance. Our project page: <https://amap-eai.github.io/SocialNav/>

1. Introduction

As embodied agents become increasingly integrated into everyday social environments, robotic navigation must prioritize not only operational efficiency but also social awareness to ensure safety and compliance with established social

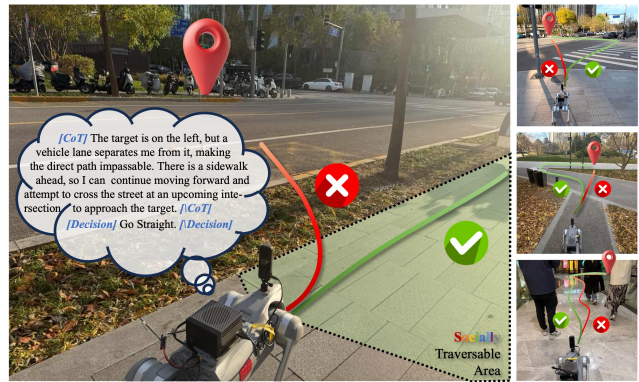


Figure 1. **Socially-Aware Navigation in Real-World Environments.** SocialNav combines high-level semantic reasoning with low-level trajectory generation. It identifies socially traversable zones and generates CoT explanations, planning routes that respect social norms.

norms. However, most existing approaches [24, 34, 35, 38, 40] focus primarily on shortest-path planning and collision avoidance, while overlooking the social compliance essential to real-world deployment (e.g., a robotic guide dog). Consequently, trajectories that appear optimal from a geometric or efficiency perspective may still lead to socially disruptive or inappropriate behaviors, such as jaywalking and traversing restricted zones (e.g., landscaped lawns).

To bridge this gap, we propose **SocialNav**, a hierarchical foundation model for socially aware navigation that integrates the understanding of social norms with the generation of socially compliant trajectories. SocialNav consists of two core components: (1) the Brain Module, built upon a vision-language model (VLM), which encodes rich social navigation priors and is capable of generating interpretable chain-of-thought (CoT) explanations or explicitly predicting socially traversable regions; and (2) the Action Expert, based on conditional flow matching [21], which

*Equal contribution.

†Corresponding author (chuzedong.cz@alibaba-inc.com)

translates the semantic priors provided by the Brain Module into robot-executable trajectories that adhere to social norms.

Developing such a model requires rich, multimodal data that encodes both cognitive knowledge and action-oriented intuition that are currently scarce in existing embodied navigation corpora. To this end, we construct the SocNav Dataset, a large-scale heterogeneous corpus of 7 million samples that integrates two complementary modalities: (1) the Cognitive Activation Dataset (CAD), which encapsulates navigational knowledge through chain-of-thought (CoT) reasoning, social traversability prediction, and embodied question answering; and (2) the Expert Trajectories Pyramid (ETP), which aggregates trajectories from internet videos, simulated environments, and real-world robot deployments to distill rich, context-aware action priors tailored for complex social navigation scenarios.

As is widely recognized, aligning agent behavior with social norms goes beyond the representational and reasoning capabilities of standard imitation learning. Even when social priors are implicitly embedded in demonstration data, behavior cloning fails to capture the causal structure underlying normative conduct. To address this limitation, we propose Socially-Aware Flow Exploration GRPO (SAFE-GRPO), the first flow-based reinforcement learning framework for embodied navigation that explicitly promotes socially compliant behavior through norm-aware reward mechanisms. This approach enables agents to internalize the underlying principles governing social conventions, rather than merely mimicking surface-level actions.

Finally, we introduce the SocNav Benchmark, a high-fidelity evaluation platform blending physics simulation (Isaac Sim [27]) and photorealistic rendering (3DGS [18]) in 9 newly captured large-scale social scenes. Our benchmark enables comprehensive comparisons of both fundamental navigation capabilities and social compliance. Our contributions are summarized as follows:

- **SocialNav Foundation Model:** a hierarchical brain–action architecture that unifies high-level social norm understanding with the generation of norm-compliant trajectories.
- **SAFE-GRPO RL Framework:** the first flow-based RL framework for embodied navigation designed to enforce social compliance through norm-aware reward shaping.
- **SocNav Dataset & Benchmark:** an integrated system featuring a large-scale cognition–action dataset and a high-fidelity evaluation platform built on Isaac Sim and 3DGS, providing comprehensive support for training and evaluating socially intelligent navigation models.

Extensive experiments on different benchmarks show that **SocialNav** significantly outperforms state-of-the-art baselines in open-loop, closed-loop, and real-world evaluation. Crucially, it demonstrates superior social compliance,

taking a meaningful stride towards true embodied social intelligence.

2. Related Work

2.1. Visual Navigation

Visual navigation [3] has evolved from classical SLAM-based methods [4, 17, 41, 42] to end-to-end learning approaches such as GNM [34], ViNT [35], and NoMaD [40]. To improve generalization, a line of work has expanded training corpora beyond expert demonstrations. Some methods, such as CityWalker [24] and MBRA [14], leverage massive internet-sourced video collections to capture diverse action priors, while others [8, 12] employ simulation platforms [32, 48] to generate controlled, rule-compliant trajectories at scale. Concurrently, VLMs are used to enhance semantic understanding [9, 29, 46, 49, 51]. However, these directions still struggle with high-level reasoning and alignment with human values in socially complex scenarios.

2.2. Social Navigation and Human Preference Alignment

Social navigation requires adherence to social conventions, moving beyond early handcrafted costs [7, 31] to VLM-based reasoning [19, 25, 45]. However, VLM reasoning is often disconnected from low-level action generation. Recently, flow matching (FM) [21] has been widely adopted in vision-and-language-action (VLA) models [15, 50] for its ability to model multimodal action distributions, but these models are typically limited to behavior cloning. In the navigation domain, pure imitation learning often lacks the causal understanding needed to robustly adapt to novel or dynamic social situations. Therefore, there is an inherent need for models that can not only generate actions but also align with complex human preferences and social norms. Foundational work, such as GRPO [10, 37] and Flow-GRPO [23], demonstrates combining generative models with online RL for human preference alignment, inspiring our approach.

3. SocNav Dataset and Benchmark

To enable the development and evaluation of socially-aware embodied navigation systems, we introduce the **SocNav Dataset** and the **SocNav Bench**. Together, they form a comprehensive ecosystem for training, validating, and benchmarking embodied agents.

3.1. SocNav Dataset

We present the **SocNav Dataset**, a large-scale, multi-source heterogeneous dataset to support robust, generalizable, and socially-aware navigation. Comprising over **7 million** training samples, the SocNav Dataset consists of two core components: the Expert Trajectories Pyramid (ETP) for learn-

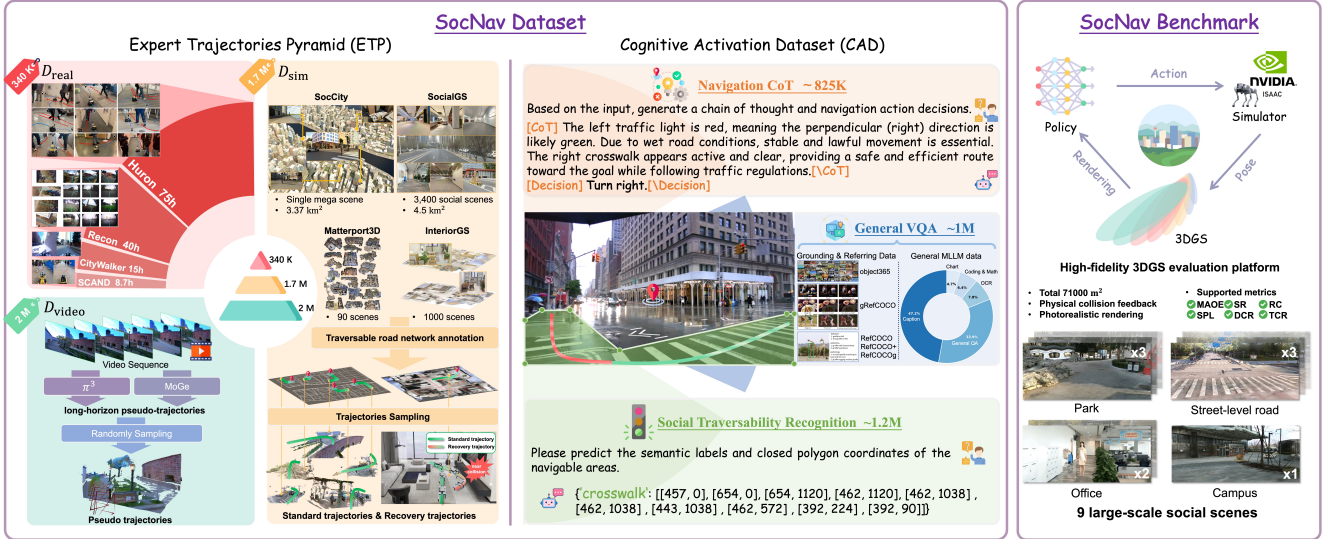


Figure 2. **Overview of the SocNav Dataset and Benchmark.** The SocNav Dataset (left) illustrates the hierarchical structure and data construction pipeline, composed of the Expert Trajectories Pyramid (ETP) and Cognitive Activation Dataset (CAD). The SocNav Benchmark (right) is a high-fidelity evaluation platform featuring large-scale, diverse social environments and offering comprehensive metrics to assess socially-aware navigation performance.

ing motion priors and the Cognitive Activation Dataset (CAD) for developing high-level reasoning.

Expert Trajectories Pyramid (ETP). The ETP is organized as a three-layer hierarchical data pyramid, covering trajectories from diverse indoor spaces (e.g., homes, offices, malls) and outdoor urban scenes (e.g., streets, parks, open areas). We define a training trajectory sample as a point-goal navigation instance. As illustrated in Figure 2, ETP consists of:

- **Trajectories from internet video (D_{video}).** D_{video} , the foundational layer, comprises **2.0 million** pseudo-trajectories, meticulously curated from extensive public urban exploration videos to ensure vast visual diversity across global cities, weather conditions, and architectural styles. These raw video streams are transformed into pseudo-trajectories via a scalable pipeline, involving: (1) Dense 3D reconstruction using π^3 [47], (2) Metric scale alignment through MoGe [44], and (3) Pseudo-trajectory synthesis by sampling diverse point-goal episodes along the reconstructed paths.
- **Trajectories from High-Fidelity Simulated Scenes (D_{sim}).** This middle data layer provides 1.7 million diverse trajectories. It comprises over **4,490** high-fidelity 3D scenes and a large-scale dynamic city. Our primary contributions to this layer are: (1) **SocialGS**, a new dataset of **3,400** real-world scenes (4.5 km²) reconstructed via 3DGS. It diversifies beyond existing residential datasets (e.g., Matterport3D [30], InteriorGS [39]) by covering social environments like shopping malls, streets, and offices. (2) **SocCity**, a **3.37 km²** dynamic urban scene

with simulated vehicles and pedestrians in Isaac Sim. Across all scenes, trajectories are generated on manually annotated traversable road networks. These trajectories encompass not only standard on-road navigation but also challenging recovery scenarios, such as near-collisions. This rich dataset enables the model to learn both efficient navigation and robust recovery behaviors.

- **Trajectories from real-world robot data (D_{real}).** This layer provides **340K** high-quality trajectories collected from autonomous robots deployed in real-world environments (from public datasets including SCAND [16], Huron [13], Recon [33], and CityWalker teleoperation data [24]). These trajectories provide ground-truth metric accuracy, physical realism, and sensor consistency, capturing true physical dynamics, sensor noise, and environmental interactions. They are ideal for supervised fine-tuning (SFT) and closing the sim-to-real gap.

Cognitive Activation Dataset (CAD). To cultivate advanced spatial cognition beyond geometric path planning, we introduce the Cognitive Activation Dataset (D_{cog}). It integrates a suite of non-trajectory auxiliary tasks designed to instill a semantically grounded understanding of environmental rules and human-centric norms.

- **Social Traversability Recognition:** We created a dataset of **1.2 million** samples by manually annotating polygons over socially traversable regions (e.g., sidewalks, crosswalks, park trails) in first-person images from internet video. This directly trains the model to distinguish between physically and socially acceptable paths.
- **Navigation Chain-of-Thought (CoT):** Leveraging first-



Figure 3. **SocialNav Architecture and Training Pipeline.** SocialNav adopts a hierarchical architecture, with a VLM-based Brain for high-level semantic reasoning and an action expert for generating socially compliant trajectories. We adopt a three-stage training strategy: Pre-training, Fine-tuning, and SAFE-GRPO.

person images and curated prompt templates, we prompted Qwen2.5VL-72B [1] to generate 825K Chain-of-Thought (CoT) samples. These samples, comprising step-by-step textual rationales for navigation decisions, were designed to teach the agent explicit reasoning.

- **General Visual Question Answering (VQA):** To ensure the model maintains general-world knowledge, we curated **1 million** general VQA samples from [5, 6, 11, 20, 22, 36]. This task trains the agent to reason about spatial relationships and object properties in the environment.

Together, the ETP and CAD establish the **SocNav Dataset** as a comprehensive foundation for training foundational navigation agents—unifying scale, realism, and cognition within a single, coherent data framework.

3.2. SocNav Benchmark

We introduce the **SocNav Bench**, a unified, high-fidelity evaluation platform for socially-aware navigation. It achieves a unique blend of realism by combining the physics simulation of Isaac Sim with the photorealistic rendering of 3DGS. The benchmark is built upon 9 new large-scale social scenes we captured and reconstructed using 3DGS, covering a total area of **73K** m^2 . These new scenes include diverse, human-centric environments: three parks, three street-level roads, two offices, and one campus. All evaluations employ a standardized setup: a unified Unitree Go2 robot model and a consistent locomotion policy. To enable realistic physical interaction, each 3DGS scene is converted into a mesh and imported into Isaac Sim for accurate

collision feedback. Additionally, to simulate potential dynamic collisions, digital humans are randomly introduced into the scenes. For rigorous benchmarking, we sample 10 start-goal pairs at distances of 20m and 100m within each scene, creating 20 evaluation cases per scene.

4. SocialNav Foundation Model

4.1. Problem Formulation

We formulate the foundational navigation task as a vision-based, history-conditioned point-goal navigation problem in diverse environments, similar to the setup in CityWalker [24]. At each time step t , the agent receives a sequence of recent monocular visual observations $\mathcal{O}_{t-n:t} = \{\mathcal{o}_{t-n}, \dots, \mathcal{o}_t\}$, where $\mathcal{o} \in \mathbb{R}^{H \times W \times 3}$, along with their associated 2D positional information $\mathcal{P}_{t-n:t} = \{\mathbf{p}_{t-n}, \dots, \mathbf{p}_t\}$ with $\mathbf{p} \in \mathbb{R}^2$. Given a specified 2D target location $\mathbf{g} \in \mathbb{R}^2$, the objective is to learn a policy π_θ that maps the historical observations and positions to a sequence of future actions:

$$\mathbf{A}_{t+1:t+m} = \pi_\theta(\mathcal{O}_{t-n:t}, \mathcal{P}_{t-n:t}, \mathbf{g}), \quad (1)$$

Unless otherwise specified, we set $n = 5$ and $m = 5$.

4.2. Model Overview

Our complete model architecture, illustrated in Fig. 3, adopts a hierarchical "brain-action" design for robust and socially aware embodied navigation. It consists of two tightly coupled branches with complementary roles: one for

high-level semantic understanding and the other for low-level action generation.

The Brain Module. The Brain Module serves as the cognitive core of the system, implemented as a Vision–Language Model (VLM) denoted by π_{VLM} . It performs generative, autoregressive textual reasoning to infer critical environmental semantics and can produce 3 types of interpretable outputs:

- **Socially traversable regions:** Represented as polygons, these delineate areas such as sidewalks, crosswalks, and stairs.
- **CoT reasoning:** Step-by-step textual explanations for navigational decisions.
- **VQA:** Responses to free-form questions that enhance scene understanding.

By explicitly generating textual outputs, the VLM provides interpretable insights essential for safe and socially responsible navigation. This design enables the agent not only to *see* but also to *reason about* its surroundings, forming the cognitive foundation for socially aware navigation.

The Action Expert. This action expert specializes in end-to-end trajectory generation. Inspired by recent advancements [2, 15] in action prediction, we leverage conditional flow matching [21] to model a distribution of actions. The module is conditioned on latent semantic features extracted from the last-layer features of the VLM:

$$\mathbf{A}_{t+1:t+m} = \pi_{\text{flow}}(\mathbf{x}_t, t; \mathbf{Z}_{\text{VLM}}) \quad (2)$$

$$\mathbf{Z}_{\text{VLM}} = \pi_{\text{VLM}}(\mathbf{O}_{t-n:t}, \mathbf{P}_{t-n:t}, \mathbf{g}) \quad (3)$$

This mechanism enables the action expert to produce efficient and socially compliant trajectories in complex environments by decoupling high-level reasoning from low-level control while preserving a strong semantic connection between them.

4.3. Training Methodology

Our training pipeline follows a multi-stage strategy designed to progressively instill both general navigation priors and social compliance into SocialNav.

Stage 1: Pre-training for General Navigation Ability.

In the first stage, we aim to activate the VLM’s navigation capability and train the flow model to predict low-level waypoints. This is achieved through pretraining on the ETP datasets (D_{video} and D_{sim}) together with the cognitive activation dataset D_{cog} . D_{video} provides diverse real-world navigation scenarios with implicit expert behaviors, while D_{sim} introduces challenging synthetic cases to enhance robustness in rare and complex situations. The D_{cog} further improves the VLM’s reasoning and decision-making through CoT and VQA tasks, and equips it with the ability to predict traversable regions—laying a solid foundation for subsequent social-norm alignment.

Stage2: Fine-tuning with High-Quality Real-World Data.

In the second stage, we fine-tune the model on high-quality expert trajectories collected from real-world robots (D_{real}) to reduce the sim-to-real gap. During this phase, the VLM is frozen, and only the action expert is optimized. This approach preserves the VLM’s semantic and social reasoning capabilities while allowing the flow model to adapt to real-world dynamics and spatial scales.

Stage3: Reinforcement Learning for Social Rule Alignment.

Although the previous stages equip the model with strong navigation priors and real-world adaptability, imitation learning still lacks causal reasoning in social environments. We therefore introduce **SAFE-GRPO** (Socially-Aware Flow Exploration GRPO), a reinforcement learning stage that explicitly aligns the policy with human social conventions. The model is trained using expert trajectories from the SocCity within D_{sim} , which provides accurate and rich pathway annotations crucial for precise reward feedback.

To encourage diverse yet meaningful exploration, we draw inspiration from the flow-based formulation of *Flow-GRPO* [23, 43], converting the deterministic ordinary differential equation (ODE) of the flow policy into a stochastic differential equation (SDE):

$$d\mathbf{x}_t = \mathbf{v}_{\text{flow}}(\mathbf{x}_t, t; \mathbf{Z}_{\text{VLM}})dt + \sigma_t d\mathbf{w}_t, \quad (4)$$

where σ_t controls the exploration magnitude. Here, \mathbf{v}_{flow} represents the velocity field of the flow policy, which is conditioned on both the current state \mathbf{x}_t and time t , as well as additional context \mathbf{Z}_{VLM} provided by the VLM.

Unlike unstructured stochastic exploration, our approach is controlled and semantically grounded: randomness is introduced only during flow integration, while the semantic conditioning signal derived from the VLM “Brain” remains fixed throughout. This latent prior encodes high-level spatial and social cues. Without explicit comprehension of scene semantics and walkable areas, conventional RL agents struggle to formulate or discover socially-compliant behaviors solely from inefficient exploration and sparse rewards.

Trajectories that are collision-free and socially valid receive higher rewards, reinforcing alignment between action generation and human expectations. The overall reward balances social compliance and navigational efficiency:

$$\mathcal{R} = \mathcal{R}_{\text{social}} + \lambda_{\text{expert}} \mathcal{R}_{\text{expert}} + \lambda_{\text{smooth}} \mathcal{R}_{\text{smooth}} + \lambda_{\text{eff}} \mathcal{R}_{\text{eff}}, \quad (5)$$

where $\mathcal{R}_{\text{social}}$ is the primary reward, derived from a semantic occupancy map \mathcal{M}_{occ} that encourages the agent to maintain safe clearance from all non-traversable areas, $\mathcal{R}_{\text{expert}}$ promotes consistency with expert trajectories, $\mathcal{R}_{\text{smooth}}$ enforces natural motion continuity, and \mathcal{R}_{eff} rewards efficient progress toward the goal. Together, these terms ensure

Table 1. **Open-Loop Evaluation on CityWalker Benchmark** [24]. We evaluate MAOE metric in each critical scenario for all methods. Percentages under scenarios indicate their data proportions. The "Mean" column shows scenario means averaged over six scenarios; "All" shows sample means over all data samples.

Method	Mean	Turn 8%	Crossing 12%	Detour 12%	Proximity 6%	Crowd 7%	Other 55%	All 100%
GNM [34]	16.2	31.1	14.8	<u>12.5</u>	14.7	12.8	11.0	12.1
ViNT [35]	16.5	31.1	15.4	12.9	14.8	13.3	11.6	12.6
NoMaD [40]	19.1	35.1	18.5	15.6	18.1	14.3	12.8	12.1
CityWalker [24]	<u>15.2</u>	<u>26.6</u>	<u>14.1</u>	13.9	<u>14.3</u>	<u>12.0</u>	<u>10.4</u>	<u>11.5</u>
SocialNav (Full)	10.2	20.1	8.8	8.4	8.9	7.6	7.2	7.8

Table 2. **Performance Comparison on the Closed-Loop SocNav Benchmark.**

Methods	Navigation Performance			Social Compliance	
	SR \uparrow	RC \uparrow	SPL \uparrow	DCR \uparrow	TCR \uparrow
GNM* [34]	43.3	62.4	37.0	26.5	28.7
ViNT* [35]	45.6	<u>66.2</u>	39.5	31.4	33.8
NoMaD* [40]	41.1	60.5	35.4	29.5	31.6
CityWalker [24]	<u>47.8</u>	64.7	<u>44.7</u>	<u>36.1</u>	<u>36.6</u>
SocialNav*	65.0	78.4	62.3	58.0	56.7
SocialNav (Full)	86.1	91.2	77.4	82.5	82.9

that the agent navigates effectively while remaining socially compliant and human-aligned. Detailed formulations are provided in the Appendix.

5. Experiment

To ensure a fair comparison, we evaluate SocialNav in three distinct settings: (1) open-loop benchmark proposed by CityWalker [24], (2) closed-loop evaluation on our SocNav Benchmark, and (3) real-world robotic deployments.

5.1. Setup

Metrics. For open-loop evaluation, we use Maximum Average Orientation Error (MAOE) following CityWalker [24]. Closed-loop performance is measured by success rate (SR; defined as reaching within 3 meters of the goal with fewer than three collisions), route completion (RC), and success weighted by path length (SPL). To assess social compliance, we introduce the Distance Compliance Rate (DCR) and Time Compliance Rate (TCR):

$$\text{DCR} = \begin{cases} \frac{d_{\text{compliant}}}{d_{\text{actual}}}, & \text{if } s = 1 \\ 0, & \text{otherwise} \end{cases} \quad (6)$$

where s is a binary indicator (1 for success, 0 for failure), $d_{\text{compliant}}$ denotes the distance traveled within socially compliant regions, and d_{actual} represents the total actual distance traveled. The TCR is formulated similarly.

Model Details. We employ Qwen2.5-VL (3B) as the brain module. The action expert is designed as a Diffusion Transformer [28] with $L = 12$ layers, $H = 12$ attention heads per layer, and hidden dimension $D = 1536$. During inference, the trajectory denoising is performed iteratively for $K = 5$ steps.

Training Details. Pre-training Stage: The full model is trained end-to-end using AdamW [26] (3 epochs, 96 H20 GPUs) with a batch size of 192 and a learning rate of 5×10^{-5} . Finetuning Stage: Only the action expert is finetuned on 32 H20 GPUs with a batch size of 256 and a learning rate of 1×10^{-5} . SAFE-GRPO: We further optimize the action expert on 16 H20 GPUs, using a rollout batch size of 128 and a learning rate of 5×10^{-7} .

5.2. Baselines

We compare SocialNav against state-of-the-art (SOTA) open-source point-based navigation methods. The selected baselines include CityWalker [24], ViNT [35], GNM [34], and NoMaD [40]. While ViNT, GNM, and NoMaD were originally designed for image-goal navigation, we re-trained them for point-goal tasks to ensure a fair comparison. In Tab. 2 and Tab. 3, an asterisk (*) denotes the models that were exclusively trained on the D_{real} dataset.

5.3. Results on CityWalker Benchmark

We evaluate on the open-loop benchmark introduced by CityWalker [24]. As shown in Tab. 1, our approach con-



Figure 4. **Qualitative comparison on the SocNav Benchmark.** We visualize representative trajectories in three scenes (Crossing, Park, Campus). The left column shows top-down path views with our method (green) and the CityWalker baseline (red), where warning signs mark unsafe or socially improper behaviors. The right columns depict corresponding egocentric views: SocialNav remains on sidewalks and walkways, while the baseline often takes shorter but socially risky routes through restricted regions (such as driveways, dry streambeds, lawns, and green belts) or crashes into obstacles like glass walls and trees.

sistently outperforms prior methods across key scenarios, demonstrating improved generalization and robustness. Since ground truth trajectories are human-operated, these results indicate that our method more closely aligns with human social walking norms.

5.4. Results on our SocNav Benchmark

We conduct closed-loop evaluation on our SocNav Benchmark, with all environments **unseen during training**. Quantitative results are shown in Tab. 2 and qualitative visualizations in Fig. 4.

Navigation Performance. SocialNav achieves state-of-the-art results across all navigation metrics. Specifically, it significantly outperforms CityWalker [24], the second-best method, with the concurrent increase of +38.3 in SR, +26.5 in RC and +32.7 in SPL.

Social Compliance. SocialNav achieves remarkable improvements in social compliance, attaining a DCR of 82.5 and a TCR of 82.9, both more than double those of CityWalker (DCR: 36.1, TCR: 36.6), and significantly better than other baselines. Representative qualitative visualizations in Fig. 4 further highlight these advantages: SocialNav consistently selects paths that adhere to sidewalks and

designated walkways, whereas the baseline frequently opts for shorter but socially inappropriate routes traversing restricted areas. This substantial improvement validates our model’s ability to internalize complex social norms. Importantly, these gains in social compliance are attained without sacrificing navigation performance.

Effect of Our Model design. The SocialNav* and baselines (including NoMaD*, GNM*, ViNT*) are trained with Imitation Learning (IL) solely on D_{real} . As shown in Tab. 2, SocialNav* significantly outperforms the baselines, clearly demonstrating the effectiveness and superior generalization capability of our model architecture.

Table 3. **Real-world Results.** Comparison of success rates across different real-world environments.

Method	Street Crossing	Office Park	Shopping Mall	Average SR
GNM* [34]	9/20	10/20	8/20	45.0
ViNT* [35]	7/20	12/20	8/20	45.0
NoMaD* [40]	9/20	11/20	10/20	50.0
CityWalker [24]	12/20	13/20	12/20	62.5
SocialNav (Full)	18/20	16/20	17/20	85.0

Table 4. **Ablation Study on Data Composition and Training Stages.** IL: Imitation Learning (Stages 1–2); RL: SAFE-GRPO (Stage 3). SocialNav* is trained with IL only on D_{real} .

No.	Model	D_{real}	D_{video}	D_{sim}	D_{cog}	IL	RL	SR \uparrow	RC \uparrow	SPL \uparrow	DCR \uparrow	TCR \uparrow
1	SocialNav*	✓				✓		65.0	78.4	62.3	58.0	56.7
2	+ D_{video}	✓	✓			✓		76.7	84.8	70.1	62.9	64.6
3	+ D_{sim}	✓	✓	✓		✓		82.2	86.0	<u>77.8</u>	69.8	68.2
4	+ D_{cog}	✓	✓	✓	✓	✓		<u>84.4</u>	88.1	79.4	<u>78.2</u>	<u>78.4</u>
5	+ RL (no D_{cog})	✓	✓	✓		✓	✓	80.0	<u>89.1</u>	78.9	68.1	66.9
6	+ RL (full data)	✓	✓	✓	✓	✓	✓	86.1	91.2	77.4	82.5	82.9

5.5. Results on the Real-World Deployments

We deploy different methods on a cloud server with an NVIDIA A10 GPU to guide a Unitree Go2 robot’s navigation. We evaluate their performance on a set of point-goal navigation tasks across three distinct environments: (1) a street crossing, (2) an office park, and (3) a shopping mall. To ensure a fair comparison, we conduct 20 trials in each environment, using the same starting and ending points for all methods. As shown in Tab. 3, SocialNav achieves a SR of 85, significantly outperforming both NoMaD [40] (50) and CityWalker [24] (62.5). Notably, SocialNav attains 18/20 successful trials in the street crossing environment, reflecting robust behavior in challenging, socially constrained settings. Additionally, SocialNav operates at over 5 Hz during deployment, enabling real-time navigation.

5.6. Ablation Studies

Effect of Data Composition. To dissect the impact of various data components on SocialNav’s performance, we conduct an ablation study by progressively adding D_{video} , D_{sim} , and D_{cog} into the IL pipeline (No. 1–4 in Tab. 4).

- **Effect of D_{video} (No.2 vs. No.1):** Large-scale Internet trajectories provide diverse human motion patterns, yielding clear gains in navigation performance (SR +11.7, RC +6.4, SPL +7.8) and improvements in social compliance (DCR +4.9, TCR +7.9).
- **Effect of D_{sim} (No.3 vs. No.2):** Expert recovery trajectories from simulation considerably strengthen robustness, leading to further improvements in SR (+5.5), RC (+1.2) and SPL (+7.7), along with moderate gains in social compliance.
- **Effect of D_{cog} (No.4 vs. No.3):** Incorporating D_{cog} yields a significant increase in social compliance rates (DCR +8.4, TCR +10.2), along with gains in overall navigation metrics. This confirms that social cognitive knowledge, by enabling CoT reasoning and traversable area prediction, is critical for the model to internalize social rules.

Effect of RL training.

- **Effect of SAFE-GRPO (No.6 vs. No.4):** Building on IL, SAFE-GRPO significantly improves social compliance,

improving DCR from 78.2 to 82.5 and TCR from 78.4 to 82.9. It also enhances navigation performance, achieving the highest SR 86.1 and RC 91.2. This demonstrates that flow-based RL with norm-aware rewards is effective for refining socially acceptable behaviors.

- **The Crucial Role of D_{cog} in RL (No.5 vs. No.3 & No.6):** Applying SAFE-GRPO without cognitive priors (No.5) worsens social metrics than IL-only training (with DCR -1.7 and TCR -1.3). This reveals a crucial insight: without the high-level social understanding encoded in D_{cog} , the RL agent lacks the foundational “brain” knowledge necessary to properly align its policy optimization with human social norms. Conversely, combining D_{cog} with SAFE-GRPO (No.6) yields the best social compliance across all settings, confirming that cognitive activations serve as essential high-level guidance for aligning RL policy improvement with human social expectations.
- **Trade-offs in Path Efficiency (No.6 vs. No.4):** We observe a minor drop in SPL (79.4→77.4) after RL. This reflects a fundamental trade-off: socially compliant behaviors (e.g., following walkways, avoiding restricted regions) are often less geometrically direct. SAFE-GRPO prioritizes human-like behaviors over shortest-path efficiency, aligning with real-world navigation norms.

6. Conclusion

In this work, we presented **SocialNav**, a hierarchical foundation model capable of socially aware embodied navigation. While SocialNav provides a scalable and generalizable framework for socially intelligent navigation, several directions remain for future exploration. First, our reinforcement learning paradigm could be extended beyond semantic traversability to capture a broader range of context-dependent human conventions. Second, the current reward formulation relies on hand-crafted rules; integrating vision-language models to deliver richer, more adaptive reward signals represents a promising step toward stronger human alignment. We believe this work marks an important milestone toward embodied agents that can navigate complex, dynamic social environments with genuine social awareness.

References

- [1] Shuai Bai, Keqin Chen, Xuejing Liu, Jialin Wang, Wenbin Ge, Sibao Song, Kai Dang, Peng Wang, Shijie Wang, Jun Tang, et al. Qwen2. 5-vl technical report. *arXiv preprint arXiv:2502.13923*, 2025. 4
- [2] Kevin Black, Noah Brown, Danny Driess, Adnan Esmail, Michael Equi, Chelsea Finn, Niccolo Fusai, Lachy Groom, Karol Hausman, Brian Ichter, et al. π_0 : A vision-language-action flow model for general robot control. corr, abs/2410.24164, 2024. doi: 10.48550. *arXiv preprint ARXIV.2410.24164*, 2024. 5
- [3] Francisco Bonin-Font, Alberto Ortiz, and Gabriel Oliver. Visual navigation for mobile robots: A survey. *Journal of intelligent and robotic systems*, 53(3):263–296, 2008. 2
- [4] Cesar Cadena, Luca Carlone, Henry Carrillo, Yasir Latif, Davide Scaramuzza, José Neira, Ian Reid, and John J Leonard. Past, present, and future of simultaneous localization and mapping: Toward the robust-perception age. *IEEE Transactions on robotics*, 32(6):1309–1332, 2017. 2
- [5] Jerun Chen, Fangyun Wei, Jinjing Zhao, Sizhe Song, Bohuai Wu, Zhuoxuan Peng, S-H Gary Chan, and Hongyang Zhang. Revisiting referring expression comprehension evaluation in the era of large multimodal models. In *Proceedings of the Computer Vision and Pattern Recognition Conference*, pages 513–524, 2025. 4
- [6] Jiu hai Chen, Le Xue, Zhiyang Xu, Xichen Pan, Shusheng Yang, Can Qin, An Yan, Honglu Zhou, Zeyuan Chen, Lifu Huang, et al. Blip3o-next: Next frontier of native image generation. *arXiv preprint arXiv:2510.15857*, 2025. 4
- [7] Yu Fan Chen, Michael Everett, Miao Liu, and Jonathan P. How. Socially aware motion planning with deep reinforcement learning. In *Proceedings of the IEEE/RSJ International Conference on Intelligent Robots and Systems (IROS)*, 2017. 2
- [8] An-Chieh Cheng, Yandong Ji, Zhaojing Yang, Zaitian Gongye, Xueyan Zou, Jan Kautz, Erdem Bıyık, Hongxu Yin, Sifei Liu, and Xiaolong Wang. Navila: Legged robot vision-language-action model for navigation. *arXiv preprint arXiv:2412.04453*, 2024. 2
- [9] An-Chieh Cheng, Yandong Ji, Zhaojing Yang, Zaitian Gongye, Xueyan Zou, Jan Kautz, Erdem Bıyık, Hongxu Yin, Sifei Liu, and Xiaolong Wang. Navila: Legged robot vision-language-action model for navigation. In *RSS*, 2025. 2
- [10] Daya Guo, Dejian Yang, Haowei Zhang, Junxiao Song, Ruoyu Zhang, Runxin Xu, Qihao Zhu, Shirong Ma, Peiyi Wang, Xiao Bi, et al. Deepseek-r1: Incentivizing reasoning capability in llms via reinforcement learning. *arXiv preprint arXiv:2501.12948*, 2025. 2
- [11] Jiawei Guo, Tianyu Zheng, Yizhi Li, Yuelin Bai, Bo Li, Yubo Wang, King Zhu, Graham Neubig, Wenhua Chen, and Xiang Yue. Mammoth-vl: Eliciting multimodal reasoning with instruction tuning at scale. In *Proceedings of the 63rd Annual Meeting of the Association for Computational Linguistics (Volume 1: Long Papers)*, pages 13869–13920, 2025. 4
- [12] Honglin He, Yukai Ma, Wayne Wu, and Bolei Zhou. From seeing to experiencing: Scaling navigation foundation models with reinforcement learning, 2025. 2
- [13] Noriaki Hirose, Dhruv Shah, Ajay Sridhar, and Sergey Levine. Sacson: Scalable autonomous control for social navigation. *IEEE Robotics and Automation Letters*, 9(1):49–56, 2023. 3
- [14] Noriaki Hirose, Lydia Ignatova, Kyle Stachowicz, Catherine Glossop, Sergey Levine, and Dhruv Shah. Learning to drive anywhere with model-based reannotation, 2025. 2
- [15] Physical Intelligence, Kevin Black, Noah Brown, James Darpinian, Karan Dhabalia, Danny Driess, Adnan Esmail, Michael Equi, Chelsea Finn, Niccolo Fusai, Manuel Y. Galliker, Dibya Ghosh, Lachy Groom, Karol Hausman, Brian Ichter, Szymon Jakubczak, Tim Jones, Liyiming Ke, Devin LeBlanc, Sergey Levine, Adrian Li-Bell, Mohith Mothukuri, Suraj Nair, Karl Pertsch, Allen Z. Ren, Lucy Xiaoyang Shi, Laura Smith, Jost Tobias Springenberg, Kyle Stachowicz, James Tanner, Quan Vuong, Homer Walke, Anna Walling, Haohuan Wang, Lili Yu, and Ury Zhilinsky. $\pi_{0.5}$: a vision-language-action model with open-world generalization, 2025. 2, 5
- [16] Haresh Karnan, Anirudh Nair, Xuesu Xiao, Garrett Warnell, Sören Pirk, Alexander Toshev, Justin Hart, Joydeep Biswas, and Peter Stone. Socially compliant navigation dataset (scand): A large-scale dataset of demonstrations for social navigation. *IEEE Robotics and Automation Letters*, 7(4):11807–11814, 2022. 3
- [17] Iman Abaspor Kazerouni, Luke Fitzgerald, Gerard Dooly, and Daniel Toal. A survey of state-of-the-art on visual slam. *Expert Systems with Applications*, 205:117734, 2022. 2
- [18] Bernhard Kerbl, Georgios Kopanas, Thomas Leimkühler, and George Drettakis. 3d gaussian splatting for real-time radiance field rendering. *ACM Trans. Graph.*, 42(4):139–1, 2023. 2
- [19] Bingqian Lin, Yunshuang Nie, Ziming Wei, Jiaqi Chen, Shikui Ma, Jianhua Han, Hang Xu, Xiaojun Chang, and Xiaodan Liang. Navcot: Boosting llm-based vision-and-language navigation via learning disentangled reasoning. *IEEE Transactions on Pattern Analysis and Machine Intelligence*, 2025. 2
- [20] Tsung-Yi Lin, Michael Maire, Serge Belongie, James Hays, Pietro Perona, Deva Ramanan, Piotr Dollár, and C Lawrence Zitnick. Microsoft coco: Common objects in context. In *European conference on computer vision*, pages 740–755. Springer, 2014. 4
- [21] Yaron Lipman, Ricky TQ Chen, Heli Ben-Hamu, Maximilian Nickel, and Matt Le. Flow matching for generative modeling. *arXiv preprint arXiv:2210.02747*, 2022. 1, 2, 5
- [22] Chang Liu, Henghui Ding, and Xudong Jiang. Gres: Generalized referring expression segmentation. In *Proceedings of the IEEE/CVF conference on computer vision and pattern recognition*, pages 23592–23601, 2023. 4
- [23] Jie Liu, Gongye Liu, Jiajun Liang, Yangguang Li, Jiaheng Liu, Xintao Wang, Pengfei Wan, Di Zhang, and Wanli Ouyang. Flow-grpo: Training flow matching models via online rl, 2025. URL <https://arxiv.org/abs/2505.05470>, 2025. 2, 5
- [24] Xinhao Liu, Jintong Li, Yicheng Jiang, Niranjan Sujay, Zhicheng Yang, Juexiao Zhang, John Abanes, Jing Zhang,

- and Chen Feng. Citywalker: Learning embodied urban navigation from web-scale videos. In *Proceedings of the Computer Vision and Pattern Recognition Conference*, pages 6875–6885, 2025. 1, 2, 3, 4, 6, 7, 8, 5
- [25] Yuxing Long, Xiaoqi Li, Wenzhe Cai, and Hao Dong. Discuss before moving: Visual language navigation via multi-expert discussions. In *2024 IEEE International Conference on Robotics and Automation (ICRA)*, pages 17380–17387. IEEE, 2024. 2
- [26] Ilya Loshchilov and Frank Hutter. Decoupled weight decay regularization. *arXiv preprint arXiv:1711.05101*, 2017. 6
- [27] NVIDIA. Isaac Sim. <https://github.com/isaac-sim/IsaacSim>, 2025. Version 5.1.0, Apache License 2.0. 2
- [28] William Peebles and Saining Xie. Scalable diffusion models with transformers. In *Proceedings of the IEEE/CVF international conference on computer vision*, pages 4195–4205, 2023. 6
- [29] Abhinav Rajvanshi, Karan Sikka, Xiao Lin, Borham Lee, Han-Pang Chiu, and Alvaro Velasquez. Saynav: Grounding large language models for dynamic planning to navigation in new environments. In *Proceedings of the International Conference on Automated Planning and Scheduling*, pages 464–474, 2024. 2
- [30] Santhosh K Ramakrishnan, Aaron Gokaslan, Erik Wijmans, Oleksandr Maksymets, Alex Clegg, John Turner, Eric Undersander, Wojciech Galuba, Andrew Westbury, Angel X Chang, et al. Habitat-matterport 3d dataset (hm3d): 1000 large-scale 3d environments for embodied ai. *arXiv preprint arXiv:2109.08238*, 2021. 3
- [31] Pascal Roth, Julian Nubert, Fan Yang, Mayank Mittal, and Marco Hutter. Viplanner: Visual semantic imperative learning for local navigation. In *2024 IEEE International Conference on Robotics and Automation (ICRA)*, pages 5243–5249. IEEE, 2024. 2
- [32] Manolis Savva, Abhishek Kadian, Oleksandr Maksymets, Yili Zhao, Erik Wijmans, Bhavana Jain, Julian Straub, Jia Liu, Vladlen Koltun, Jitendra Malik, et al. Habitat: A platform for embodied ai research. In *Proceedings of the IEEE/CVF international conference on computer vision*, pages 9339–9347, 2019. 2
- [33] Dhruv Shah, Benjamin Eysenbach, Nicholas Rhinehart, and Sergey Levine. Rapid exploration for open-world navigation with latent goal models. In *Conference on Robot Learning*, pages 674–684. PMLR, 2022. 3
- [34] Dhruv Shah, Ajay Sridhar, Arjun Bhorkar, Noriaki Hirose, and Sergey Levine. Gnm: A general navigation model to drive any robot. In *ICRA*, pages 7226–7233. IEEE, 2023. 1, 2, 6, 7
- [35] Dhruv Shah, Ajay Sridhar, Nitish Dashora, Kyle Stachowicz, Kevin Black, Noriaki Hirose, and Sergey Levine. ViNT: A foundation model for visual navigation. In *CoRL*, 2023. 1, 2, 6, 7
- [36] Shuai Shao, Zeming Li, Tianyuan Zhang, Chao Peng, Gang Yu, Xiangyu Zhang, Jing Li, and Jian Sun. Objects365: A large-scale, high-quality dataset for object detection. In *Proceedings of the IEEE/CVF international conference on computer vision*, pages 8430–8439, 2019. 4
- [37] Zhihong Shao, Peiyi Wang, Qihao Zhu, Runxin Xu, Junxiao Song, Xiao Bi, Haowei Zhang, Mingchuan Zhang, Yuankai Li, Yifeng Wu, and Daya Guo. Deepseekmath: Pushing the limits of mathematical reasoning in open language models. *CoRR*, abs/2402.03300, 2024. 2
- [38] Phani Teja Singamaneni, Pilar Bachiller-Burgos, Luis J Manso, Anaís Garrell, Alberto Sanfeliu, Anne Spalanzani, and Rachid Alami. A survey on socially aware robot navigation: Taxonomy and future challenges. *The International Journal of Robotics Research*, 43(10):1533–1572, 2024. 1
- [39] Manycore Tech Inc. SpatialVerse Research Team. Interiors: A 3d gaussian splatting dataset of semantically labeled indoor scenes. <https://huggingface.co/datasets/spatialverse/InteriorGS>, 2025. 3
- [40] Ajay Sridhar, Dhruv Shah, Catherine Glossop, and Sergey Levine. Nomad: Goal masked diffusion policies for navigation and exploration. In *2024 IEEE International Conference on Robotics and Automation (ICRA)*, pages 63–70. IEEE, 2024. 1, 2, 6, 7, 8
- [41] Takafumi Taketomi, Hideaki Uchiyama, and Sei Ikeda. Visual slam algorithms: A survey from 2010 to 2016. *IPSA transactions on computer vision and applications*, 9(1):16, 2017. 2
- [42] Emmanouil G Tsardoulidis, A Iliakopoulou, Andreas Karakos, and Loukas Petrou. A review of global path planning methods for occupancy grid maps regardless of obstacle density. *Journal of intelligent & robotic systems*, 84(1):829–858, 2016. 2
- [43] Feng Wang and Zihao Yu. Coefficients-preserving sampling for reinforcement learning with flow matching, 2025. 5
- [44] Ruicheng Wang, Sicheng Xu, Cassie Dai, Jianfeng Xiang, Yu Deng, Xin Tong, and Jiaolong Yang. Moge: Unlocking accurate monocular geometry estimation for open-domain images with optimal training supervision. In *Proceedings of the Computer Vision and Pattern Recognition Conference*, pages 5261–5271, 2025. 3
- [45] Shuo Wang, Yongcai Wang, Wanting Li, Xudong Cai, Yucheng Wang, Maiyue Chen, Kaihui Wang, Zhizhong Su, Deying Li, and Zhaoxin Fan. Aux-think: Exploring reasoning strategies for data-efficient vision-language navigation. *arXiv preprint arXiv:2505.11886*, 2025. 2
- [46] Shaoan Wang, Jiazhao Zhang, Minghan Li, Jiahang Liu, Anqi Li, Kui Wu, Fangwei Zhong, Junzhi Yu, Zhizheng Zhang, and He Wang. Trackvla: Embodied visual tracking in the wild. *arXiv preprint arXiv:2505.23189*, 2025. 2
- [47] Yifan Wang, Jianjun Zhou, Haoyi Zhu, Wenzheng Chang, Yang Zhou, Zizun Li, Junyi Chen, Jiangmiao Pang, Chunhua Shen, and Tong He. π^3 : Scalable permutation-equivariant visual geometry learning. *arXiv e-prints*, pages arXiv–2507, 2025. 3
- [48] Wayne Wu, Honglin He, Chaoyuan Zhang, Jack He, Seth Z Zhao, Ran Gong, Quanyi Li, and Bolei Zhou. Towards autonomous micromobility through scalable urban simulation. In *Proceedings of the Computer Vision and Pattern Recognition Conference*, pages 27553–27563, 2025. 2
- [49] Xinda Xue, Junjun Hu, Minghua Luo, Xie Shichao, Jintao Chen, Zixun Xie, Quan Kuichen, Guo Wei, Mu Xu, and Zedong Chu. Omnnav: A unified framework for prospective

exploration and visual-language navigation. *arXiv preprint arXiv:2509.25687*, 2025. [2](#)

- [50] Kai Yang, Tianlin Zhang, Zhengbo Wang, Zedong Chu, Xiaolong Wu, Yang Cai, and Mu Xu. Ce-nav: Flow-guided reinforcement refinement for cross-embodiment local navigation. *arXiv preprint arXiv:2509.23203*, 2025. [2](#)
- [51] Jiazhao Zhang, Kunyu Wang, Rongtao Xu, Gengze Zhou, Yicong Hong, Xiaomeng Fang, Qi Wu, Zhizheng Zhang, and He Wang. Navid: Video-based vlm plans the next step for vision-and-language navigation. *arXiv preprint arXiv:2402.15852*, 2024. [2](#)

SocialNav: Training Human-Inspired Foundation Model for Socially-Aware Embodied Navigation

Supplementary Material

Content

A Supplementary Materials for the SocNav Dataset and Benchmark	1
A.1 Construction of Trajectories in D_{sim}	1
A.1.1. Standard Trajectory Generation	1
A.1.2. Recovery Trajectory Generation	1
A.1.3. Visualization of Standard and Recovery Trajectories	2
A.2 Annotation of Socially Traversable Regions	2
A.2.1. Annotation Pipeline	2
A.2.2. Annotation Guidelines	2
A.2.3. Qualitative Analysis of Social Traversability Prediction	2
A.3 Navigation Chain-of-Thought Construction	3
A.3.1. Prompt Design	3
A.3.2. Qualitative Example of Navigation CoT	3
A.4 Details of the SocNav Benchmark	5
A.4.1. Metric Definitions	5
A.4.2. Pedestrian Placement and Behavior Model	5
B Supplementary Materials for the SocialNav Foundation Model	5
B.1. Model Architecture and Parameters	5
B.2. Training Details	5
B.3. SAFE-GRPO Reward Design	6
B.4. Ablation on SAFE-GRPO Reward Functions	6
C Additional Experimental Results	6
C.1. Extended Open-Loop Results on the CityWalker Benchmark	6
C.2. Additional Real-World Deployment Visualizations	7

A. Supplementary Materials for the SocNav Dataset and Benchmark

A.1. Construction of Trajectories in D_{sim}

The simulated subset D_{sim} in the SocNav Dataset is designed to provide both *standard trajectories* and *recovery trajectories* in structured social scenes. This section details the construction pipeline and provides schematic visualizations.

A.1.1. Standard Trajectory Generation

For each scene, we first construct a navigation graph over the legal road network (sidewalks, crosswalks, plazas, etc.):

- Road network annotation.** For SocCity, we derive the traversable occupancy map M_{occ} by mapping the semantic ground annotations inherent to the 3D city assets. For other 3D scenes (SocialGS, MatterPort3D, InteriorGS), we manually annotate M_{occ} . We ensure a unified definition of traversability across all datasets (refer to Sec.A.2.2 for details). Subsequently, guided by the M_{occ} of each scene, we manually annotate the road network along the centerlines of the traversable paths.
- Trajectory Generation.** We randomly sample a start position s and a goal position g on the traversable road network, ensuring that the geodesic distance $d(s, g)$ along the network exceeds a minimum threshold $\ell_{\text{min}} = 50$ m. We then employ an A* planner to compute the shortest path, which serves as the standard trajectory τ^* . These trajectories represent ideal navigation behavior that consistently maintains a safe distance from untraversable areas.

A.1.2. Recovery Trajectory Generation

While standard trajectories provide an ideal reference, training a policy exclusively on such expert data can lead to brittleness. The agent may fail to recover from even small deviations, a classic problem of covariate shift in imitation learning. To address this and equip the agent with robust recovery capabilities, we augment the standard expert demonstrations with a set of *recovery trajectories*. These are designed to simulate scenarios where the agent starts in a sub-optimal or dangerous state and must execute a corrective maneuver to rejoin the ideal path.

The generation process for these recovery trajectories is as follows:

- Define Convergence Point.** For each standard trajectory τ^* starting at s , we first identify a convergence point p_{conv} on τ^* , located 5 meters ahead of the start point s .
- Sample Recovery Start.** We then generate a corresponding recovery start point s_{rec} by applying a random lateral offset (either left or right) to the standard start point s . To construct a challenging recovery task, the initial orientation at s_{rec} is deliberately misaligned:
 - If s_{rec} is offset to the **left**, the initial heading is set to a random angle within $[-90^\circ, -45^\circ]$ relative to the forward direction of the standard path.
 - If s_{rec} is offset to the **right**, the initial heading is set to

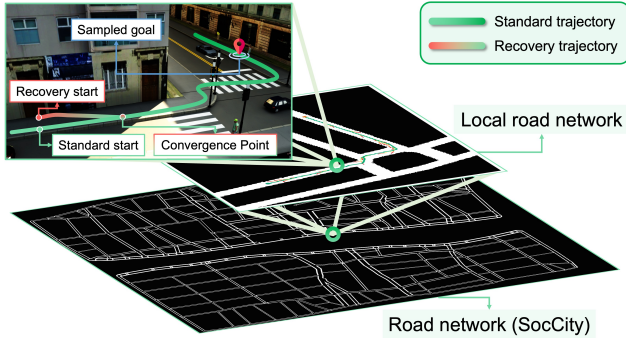


Figure 5. **Standard and recovery trajectories in D_{sim} .** Visual examples from SocCity scenes. Green curves denote standard expert trajectories obtained by A* planning on the navigation graph, while the other curves depict locally sampled recovery trajectories originating from intermediate points. The background shows the semantic occupancy map \mathcal{M}_{occ} with walkable regions (white) and non-traversable regions (black).

an angle within $[45^\circ, 90^\circ]$.

This forces the agent to start by facing away from the correct path, requiring an immediate and decisive turn.

3. **Generate Recovery Trajectory.** A dense recovery path τ^{rec} is generated by linearly interpolating between the recovery start state s_{rec} and the convergence point p_{conv} with a fixed spatial step of approximately 5 cm. To simulate natural human micro-corrections and avoid trivial straight-line paths, we perturb each interpolated point q_t with small, zero-mean Gaussian noise:

$$q'_t = q_t + \epsilon_t, \quad \epsilon_t \sim \mathcal{N}(\mathbf{0}, (0.01 \text{ m})^2 \mathbf{I}). \quad (7)$$

The final perturbed path $\tau^{rec'}$ is formed by concatenating τ^{rec} with the path from p_{conv} to g . It is kept only if all its points remain in cells of \mathcal{M}_{occ} with sufficient clearance from obstacles.

These systematically constructed recovery trajectories mimic plausible failure scenarios, such as starting from the wrong orientation or position, and provide explicit supervision on how to execute safe and efficient corrective actions. This enriches the training data far more effectively than simple random noise, significantly improving the policy’s robustness in challenging situations.

A.1.3. Visualization of Standard and Recovery Trajectories

Figure 5 illustrates typical standard and recovery trajectories on \mathcal{M}_{occ} , highlighting the diversity introduced by local recovery paths.

A.2. Annotation of Socially Traversable Regions

Socially traversable regions provide the supervision signal for training the SocialNav Brain to predict socially compli-

ant polygons. We describe the annotation pipeline and the corresponding guidelines.

A.2.1. Annotation Pipeline

1. **Internet-scale data collection.** We gather first-person Internet videos and images depicting pedestrians moving in outdoor scenes such as streets, campuses, and parks.
2. **Automatic filtering.** A vision-language model is used to filter out frames with unsuitable viewpoints (e.g., too close to walls, heavily occluded, or dominated by sky/ground) and to discard low-quality images.
3. **Manual polygon annotation.** Human annotators draw coarse polygons on the remaining frames to delineate socially traversable regions. We create one or more polygons to cover all regions that is legally and socially allowed to walk.

A.2.2. Annotation Guidelines

- **Socially Traversable Regions.** These are defined as outdoor areas where pedestrians are permitted to walk by both legal regulations and common social norms. Annotators were instructed to label surfaces such as sidewalks, pedestrian-only streets, marked crosswalks, public plazas, and accessible outdoor staircases. For indoor scenes, all non-obstacle areas are considered traversable.
- **Non-Traversable Regions.** This category encompasses all areas that are unsafe, illegal, or socially unacceptable for pedestrian traffic. Key examples include motor vehicle lanes, bike lanes, bus lanes, green belts, ornamental lawns, flower beds, water bodies, etc.
- **Annotation Protocol and Polygon Standards.** Annotators draw coarse, low-vertex polygons to cover the full extent of the walkable surface; pixel-perfect alignment with curbs or markings is not required. Annotation focuses on the walkable region directly connected to the camera’s viewpoint. A single polygon can span multiple connected surfaces (e.g., a sidewalk leading into a plaza). Isolated regions that cannot be reached without crossing non-traversable areas are ignored, except for pedestrian safety islands that are visibly reachable via crosswalks.

A.2.3. Qualitative Analysis of Social Traversability Prediction

Figure 6 presents qualitative comparisons of predicted socially traversable regions across six unseen test scenes. Each column corresponds to a different scene, while the four rows show: (1) Qwen2.5-VL predictions in SocCity, (2) SocialNav predictions in SocCity, (3) Qwen2.5-VL predictions in the real world, and (4) SocialNav predictions in the real world. Green polygons denote model-predicted socially traversable regions.

Across both simulated and real scenes, the base Qwen2.5-VL-3B model often produces polygons that are coarse, spatially misaligned, or leak into socially invalid

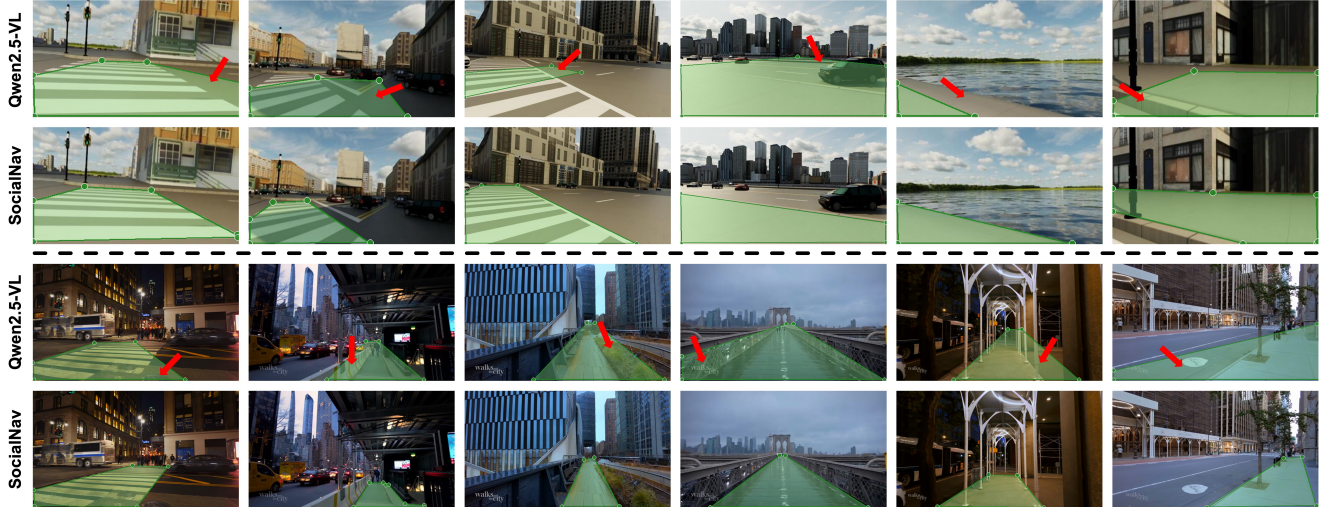


Figure 6. **Predicted socially traversable regions on unseen scenes.** Green polygons denote predicted socially traversable regions, and red arrows highlight areas incorrectly classified as traversable. SocialNav yields more semantically aligned polygons in both domains.

areas such as curb edges, grass, or vehicle lanes. In contrast, the SocialNav Brain, trained with our large-scale traversability annotations, provides predictions that are more structured and socially consistent: polygons more tightly follow sidewalks, pedestrian paths, and crosswalks, and avoid visually similar but non-walkable regions. The improvements hold across all six diverse unseen scenes, indicating that fine-tuning not only enhances accuracy but also significantly strengthens cross-domain generalization.

A.3. Navigation Chain-of-Thought Construction

To construct the Cognitive Activation Dataset (CAD) for navigation, we elicit chain-of-thought (CoT) style explanations using an instruction prompt. The goal is to obtain, for each navigation step, (i) a structured reasoning trace that explains the agent’s decision in terms of scene layout, social norms, and future consequences, and (ii) a final discrete action selected from a predefined action space. This subsection details the prompt design and the corresponding input–output specification.

A.3.1. Prompt Design

Task and Role Description. We explicitly cast the brain model as the *Thinking Module* of a professional navigation system. Its responsibility is to produce a logically coherent CoT and a final movement decision.

Then the prompt enforces a strict three-stage reasoning protocol:

1. **Global situation analysis:** jointly parse all input information, including the robot state, the target location, and visual observations.

2. **Chain-of-thought generation:** A **CoT segment**, enclosed between `[CoT]` and `[\CoT]`, containing the full reasoning process which includes structured, logically tight reasoning process that evaluates the consequences of different candidate actions under social and geometric constraints.
3. **Final decision:** A **Decision segment**, enclosed between `[Decision]` and `[\Decision]`, containing exactly one chosen action from the predefined action space.

Prompt Template. Figure 7 presents the complete English-language prompt template used to generate the navigation CoTs for our CAD. The resulting CoT and Decision segments are stored alongside the visual observations and trajectory states, forming rich supervision for the Brain Module to acquire socially aware navigation reasoning.

A.3.2. Qualitative Example of Navigation CoT

Figure 8 provides a qualitative example of the chain-of-thought (CoT) generated by our Brain Module for a navigation decision in an unseen urban intersection. The CoT showcases the model’s ability to perform complex, multi-stage reasoning by integrating its state, goal, and rich perceptual understanding.

In this example, the model correctly identifies a conflict between the long-term goal vector (to the forward-right) and the immediate safety and social constraints. Instead of pursuing a direct path, the model decomposes the problem, recognizing that the sanctioned crosswalk directly ahead, aided by a green pedestrian signal, is the necessary intermediate step. It explicitly evaluates actions against a learned hierarchy of navigational rules—1) Safety, 2) Social Compliance, and 3) Task Efficiency—to invalidate unsafe actions

Role and task description:
 You are now the *Thinking Module* of a professional navigation AI system. Your single core task is to generate, for every movement of a quadruped robot dog, a comprehensive, in-depth, and logically rigorous *Chain of Thought (CoT)*, and then output a clear movement decision. This CoT must integrate all available environmental information and explain why the final decision is the optimal choice under the current situation.

Workflow (you *must* strictly follow these three steps, without omission or reordering):
 1. Comprehensive analysis: parse all input information, including the robot's own state, the goal position, and environmental perception.
 2. CoT generation: based on your analysis, build a structured, logically sound reasoning process and evaluate all plausible alternatives.
 3. Final decision: select one and only one action from the candidate action space, and output it in the specified format.

Input information:
 1. Scene information:
 a. Format: [[history_coord.1], [history_coord.2], [history_coord.3], [history_coord.4], [current_coord], [goal_coord]] together with the corresponding observation images in the same order.
 b. Interpretation: this sequence represents the robot dog's past and current coordinates, followed by the target coordinate.
 c. Coordinate system: the positive *Y* direction corresponds to forward, and the positive *X* direction corresponds to right.

2. Candidate action space:
 -- Go Straight
 -- Stay Still
 -- Move Backward
 -- Move Forward-Left
 -- Move Forward-Right
 -- Move Left
 -- Move Right

Output requirements:
 You must generate a *single*, continuous block of text (no meaningless spaces, blank lines, or extra line breaks). Absolutely no additional explanations, headings, greetings, or apologies are allowed. You must strictly follow the format below:
 [CoT]... [\CoT][Decision]... [\Decision]

Figure 7. Navigation Chain-of-Thought Prompt Template. The full prompt used to construct the Cognitive Activation Dataset.

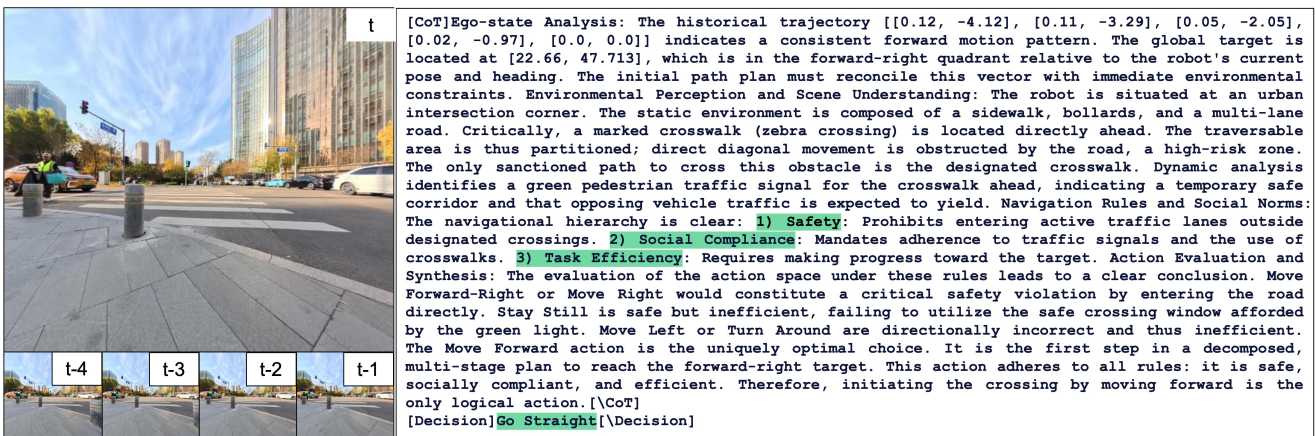


Figure 8. Example of a navigation chain-of-thought (CoT) in an unseen crossing scenario. Given the historical observations (left) and a goal in the forward-right direction, the Brain Module generates a structured CoT (right). The CoT demonstrates hierarchical decision-making, prioritizing Safety (no jaywalking) and Social Compliance (using the crosswalk) over direct path efficiency.

(e.g., Move Forward-Right) and inefficient ones (e.g., Stay Still). The final decision to Go Straight is thus not a simple reactive choice but the output of a deliber-

ate plan to safely and compliantly progress toward the goal.

A.4. Details of the SocNav Benchmark

The SocNav Benchmark provides a closed-loop evaluation platform for jointly assessing navigation performance and social compliance.

A.4.1. Metric Definitions

Standard point-goal Navigation metrics.

- **MAOE.** Following CityWalker [24], we compute the Average Orientation Error (AOE) at each prediction step k as the mean angular difference between the predicted action \hat{a}_{i_k} and the ground-truth action a_{i_k} over all samples:

$$\text{AOE}(k) = \frac{1}{n} \sum_{i=1}^n \theta_{i_k}, \quad \theta_{i_k} = \arccos \left(\frac{\langle \hat{a}_{i_k}, a_{i_k} \rangle}{\|\hat{a}_{i_k}\|_2 \|a_{i_k}\|_2} \right). \quad (8)$$

The Maximum Average Orientation Error (MAOE) aggregates over predicted horizons:

$$\text{MAOE} = \frac{1}{n} \sum_{i=1}^n \max_k \theta_{i_k}, \quad (9)$$

which emphasizes the worst-case orientation mismatch along future steps.

- **Success Rate (SR).** The fraction of episodes in which the agent reaches within 3 m of the target with fewer than three collisions.
- **Route Completion (RC).** The ratio between the geodesic distance from start to the final position and the geodesic distance from start to goal.
- **Success weighted by Path Length (SPL).** The SPL metric, as in prior navigation work, jointly captures success and path efficiency.

Social compliance metrics: DCR and TCR. The Distance Compliance Rate (DCR) measures the proportion of distance spent in socially traversable regions:

$$\text{DCR} = \begin{cases} \frac{d_{\text{compliant}}}{d_{\text{actual}}}, & \text{if } s = 1, \\ 0, & \text{otherwise,} \end{cases} \quad (10)$$

where $s \in \{0, 1\}$ indicates success, $d_{\text{compliant}}$ is the distance traveled in regions labeled as socially traversable, and d_{actual} is the total traveled distance.

The Time Compliance Rate (TCR) is defined analogously by replacing distance with duration spent in compliant regions. Both metrics are computed only for successful episodes and are averaged over all tasks.

A.4.2. Pedestrian Placement and Behavior Model

To simulate realistic social environments, we populate the evaluated scenes with dynamic pedestrians:

Table 5. Model Architecture and Parameters.

Brain Module (Qwen2.5-VL-3B)	
Layers / Hidden / MLP	36 / 2048 / 11008
Attention heads (KV)	16 (2)
Activation / Norm	SiLU / RMSNorm
Max context	128k (SW: 32k)
RoPE scaling	multi-segment (16/24/24)
Vocab size	151,673
Action Expert (Diffusion Transformer)	
Action dim / Chunk size	2 / 5
Flow-matching steps	5

- **Placement and Density.** To ensure realistic positioning, pedestrians are spawned within a specific margin, between 50 cm and 100 cm from the inner boundary of the socially traversable regions. We maintain a pedestrian density of not exceeding 6 individuals per 100 meters of walkable path.
- **Behavior model.** The behavior of each pedestrian is governed by a skeletal animation system, which supports both walking and running actions. Each pedestrian selects a random goal on the road network and moves along the shortest path at a speed sampled from a truncated normal distribution (mean 1.0 m/s, standard deviation 0.2 m/s).
- **Interaction with the robot.** Pedestrians do not explicitly cooperate with the robot; they follow their own routes. Consequently, the robot must proactively adapt its trajectory to maintain social distances and avoid intruding into non-traversable regions.

B. Supplementary Materials for the SocialNav Foundation Model

The **SocialNav** foundation model adopts the hierarchical Brain–Action design described in the main paper. Here we summarize key architectural details.

B.1. Model Architecture and Parameters

Table 5 summarizes the architectural parameters of the **Brain Module** (Qwen2.5-VL-3B) and the **Action Expert** (Diffusion Transformer). The table includes structural details necessary for reproducibility.

B.2. Training Details

This section provides concise supplementary training information for the three-stage pipeline introduced in the main paper. Table 6 summarizes both the trainable components and the datasets used in each stage, while some shared optimization settings remain unchanged across the entire pipeline.

Table 6. **Trainable Components and Datasets Across Stage 1–3.** Checkmarks indicate modules updated during each stage.

Stage	Datasets	Trainable Modules			
		VLM Brain	Vision Encoder	Waypoint Encoder	Action Expert
Pre-training	$D_{\text{video}}, D_{\text{sim}}, D_{\text{cog}}$	✓	✓	✓	✓
Fine-tuning	D_{real}	×	×	×	✓
SAFE-GRPO	$D_{\text{sim}} (\text{SocCity})$	×	×	×	✓

Table 7. **Hyperparameter Settings.**

Settings	Value
Optimizer	AdamW
Adam betas (β_1, β_2)	(0.9, 0.95)
Weight decay	0.1
LR scheduler	Cosine decay
Precision	BF16
Flash Attention 2	Enabled
Gradient accumulation	1
Gradient checkpointing	Enabled

Hyperparameter settings are summarized in Table 7.

B.3. SAFE-GRPO Reward Design

Social Compliance Reward $\mathcal{R}_{\text{social}}$: This is the primary incentive for respecting both physical safety and social norms. From $\mathcal{M}_{\text{occ}} \in \{0, 1\}^{H \times W}$, we compute a Distance Transform (DT) map $D(\mathbf{x})$, which assigns each traversable location \mathbf{x} its Euclidean distance to the nearest non-traversable cell. This DT map encodes both collision avoidance and social distancing principles—higher values indicate safer, more normatively acceptable regions.

Let $\{\mathbf{x}_t\}_{t=1}^T$ be the predicted trajectory in world coordinates, and let $\bar{d}_{\text{pred}} = \frac{1}{T} \sum_{t=1}^T D(\mathbf{x}_t)$ denotes the average obstacle-free clearance along the path. Similarly, we compute \bar{d}_{gt} for the expert trajectory. The social reward is then formulated as:

$$\mathcal{R}_{\text{social}} = \beta \cdot \sigma \left(\frac{\bar{d}_{\text{pred}} - \bar{d}_{\text{gt}}}{\alpha} \right), \quad (11)$$

where $\sigma(\cdot)$ denotes the sigmoid function, and hyperparameters $\alpha = 0.5$, $\beta = 2.0$ control sensitivity and scaling. This formulation rewards trajectories that maintain comparable or greater clearance than the expert.

Expert Trajectory Similarity Reward $\mathcal{R}_{\text{expert}}$: We measure similarity in both spatial proximity and directional consistency. Given predicted trajectory \mathbf{p} and expert \mathbf{g} in world coordinates:

$$\mathcal{R}_{\text{expert}} = w_d \cdot r_{\text{dist}} + w_\theta \cdot r_{\text{dir}}, \quad (12)$$

where:

$$r_{\text{dist}} = \exp \left(-\frac{1}{T} \sum_{t=1}^T \frac{\|\mathbf{p}_t - \mathbf{g}_t\|}{\tau_d} \right), \quad (13)$$

$$r_{\text{dir}} = \frac{1}{2} (\cos(\Delta\theta_{\text{avg}}) + 1) \in [0, 1], \quad (14)$$

with $w_d = 0.7$, $w_\theta = 0.3$, $\tau_d = 1.0$ m. Here, $\Delta\theta_{\text{avg}}$ is the average angular difference between consecutive displacement vectors.

Trajectory Smoothness Reward $\mathcal{R}_{\text{smooth}}$: We encourage consistent step lengths by penalizing high variance in inter-step distances:

$$\mathcal{R}_{\text{smooth}} = \exp \left(-\frac{\text{std}(\{\|\Delta\mathbf{x}_t\|\}_{t=2}^T)}{\alpha_s} \right), \quad (15)$$

where $\alpha_s = 0.8$, and $\text{std}(\cdot)$ computes the standard deviation of step magnitudes. A lower variance yields higher reward, promoting natural gait-like movement.

Path Efficiency Reward $\mathcal{R}_{\text{efficiency}}$: To encourage forward progress without excessive detours, we compare the agent’s net advancement to that of the expert:

$$\mathcal{R}_{\text{efficiency}} = \beta_l \cdot \sigma \left(\frac{\|\mathbf{x}_T - \mathbf{x}_0\|_2 - \|\mathbf{x}_T^{\text{gt}} - \mathbf{x}_0^{\text{gt}}\|_2}{\alpha_l} \right), \quad (16)$$

where $\alpha_l = 5.0$, $\beta_l = 2.0$. By combining these reward components, our design ensures that the agent learns to navigate not only effectively, but also in a manner that is predictable, respectful, and aligned with human expectations within shared environments.

B.4. Ablation on SAFE-GRPO Reward Functions

We ablate the $\mathcal{R}_{\text{social}}$ defined in Eq. (4) of the main paper. For the variant, we set the weight of the $\mathcal{R}_{\text{social}}$ to zero while keeping all other training configurations unchanged.

The results in Table 8 show that $\mathcal{R}_{\text{social}}$ is crucial for high DCR and TCR; without it, the agent tends to take shorter but socially risky shortcuts.

C. Additional Experimental Results

C.1. Extended Open-Loop Results on the CityWalker Benchmark

We provide an extended comparison on the CityWalker open-loop benchmark. The model variants marked with asterisk (*) denotes the models that were exclusively trained on the D_{real} dataset.

Compared to the official CityWalker model, the retrained CityWalker* shows consistent improvements across all scenarios, confirming that our D_{real} provides a more comprehensive navigation motion priors. Similarly, GNM*, ViNT*, and NoMaD* benefit from retraining.

Table 8. **Ablation on SAFE-GRPO reward components on the SocNav Benchmark.** We deactivate each reward term in turn by setting its weight to zero. Checkmarks indicate that the reward is used.

Variant	Reward terms				SocNav Benchmark				
	$\mathcal{R}_{\text{social}}$	$\mathcal{R}_{\text{expert}}$	$\mathcal{R}_{\text{smooth}}$	$\mathcal{R}_{\text{efficiency}}$	SR \uparrow	RC \uparrow	SPL \uparrow	DCR \uparrow	TCR \uparrow
w/o $\mathcal{R}_{\text{social}}$	–	✓	✓	✓	84.7	90.3	78.5	61.4	62.1
Full SAFE-GRPO	✓	✓	✓	✓	86.1	91.2	77.4	82.5	82.9

Table 9. **Open-Loop Evaluation on CityWalker Benchmark [24].** We evaluate MAOE metric in each critical scenario for all methods. Percentages under scenarios indicate their data proportions. The "Mean" column shows scenario means averaged over six scenarios; "All" shows sample means over all data samples.

Method	Mean	Turn 8%	Crossing 12%	Detour 12%	Proximity 6%	Crowd 7%	Other 55%	All 100%
GNM* [34]	15.2	29.5	13.6	11.9	13.6	12.3	10.4	11.5
ViNT* [35]	15.8	30.0	14.6	12.3	14.0	12.7	11.0	12.2
NoMaD* [40]	17.8	33.4	16.5	14.8	16.2	13.6	12.2	12.3
CityWalker* [24]	14.2	25.0	12.8	12.5	13.2	11.5	10.0	11.2
SocialNav*	11.7	21.5	10.9	10.4	9.8	8.9	8.7	9.4
SocialNav (Full)	10.2	20.1	8.8	8.4	8.9	7.6	7.2	7.8

SocialNav (Full) achieves the lowest MAOE in every scenario and in the overall mean. The largest relative gains are observed in the *Turn* and *Crossing* categories, where understanding of social layout and high-level semantics is particularly important. This trend supports our claim that integrating the Brain Module with the flow-based Action Expert leads to trajectories that more closely match human-operated behaviors.

C.2. Additional Real-World Deployment Visualizations

To further illustrate the real-world performance of SocialNav, we visualize third-person view from the Unitree Go2 deployments described in Table 3.

The visualizations highlight that SocialNav can be executed in real-time on a cloud server with an NVIDIA A10 GPU, maintaining over 5 Hz control frequency while preferring socially acceptable walkways even when shorter but socially inappropriate shortcuts exist.

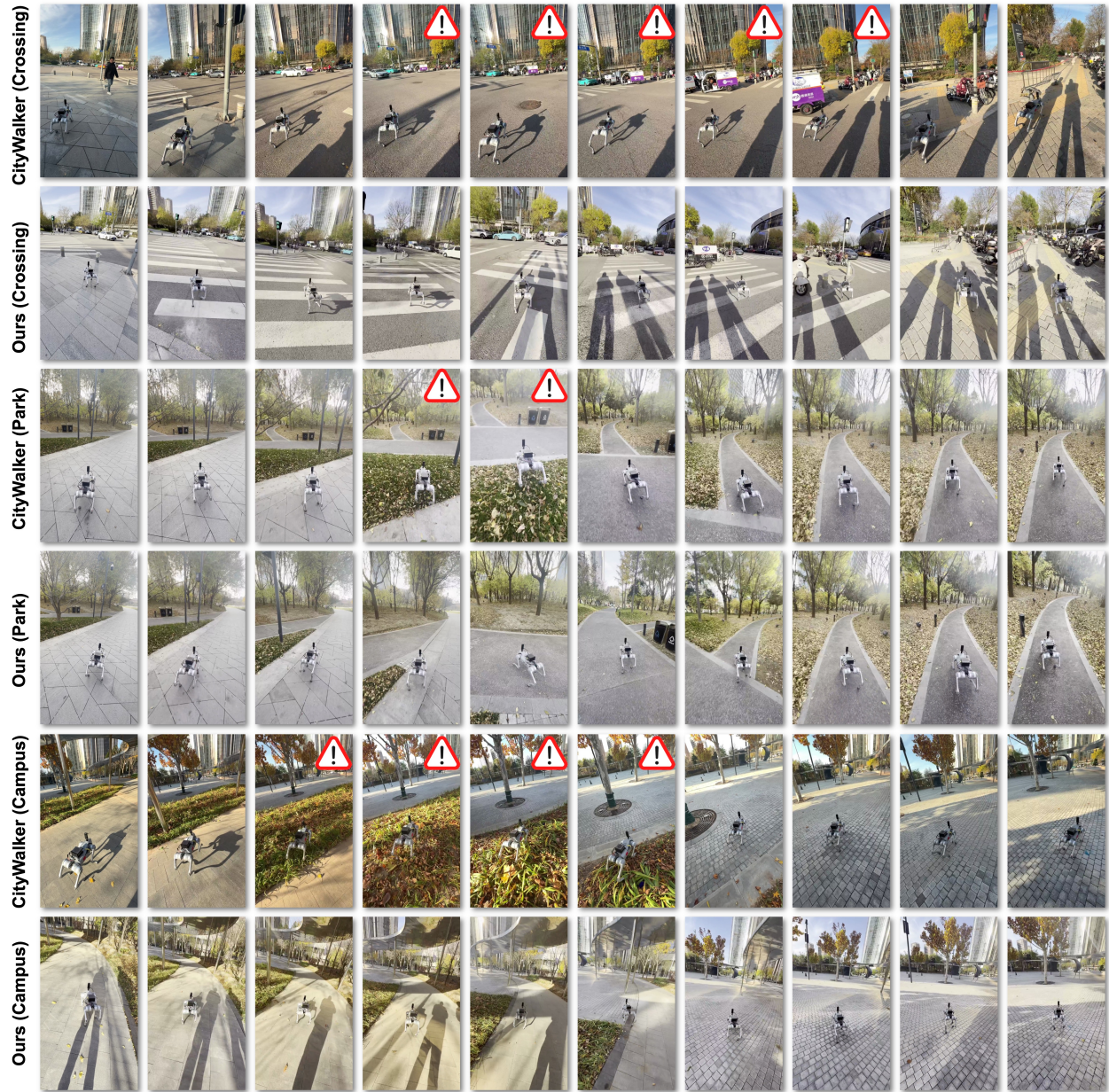


Figure 9. **Real-world deployment visualizations.** Third-person views of the Unitree Go2 robot navigating in street, park, and campus environments. SocialNav successfully follows sidewalks, avoids stepping onto lawns or driveways, respects pedestrian flows.